Journal of Power Sources 245 (2014) 203–207

Contents lists available at SciVerse ScienceDirect

Journal of Power Sources

journal homepage: www.elsevier.com/locate/jpowsour

Short communication

Oxygen permeability of cast ionomer films from chronoamperometry on microelectrodes

Jerzy Chlistunoff*

Los Alamos National Laboratory, Materials Physics and Applications Division, P.O. Box 1663, MS D429, Los Alamos, NM 87545, USA

HIGHLIGHTS

- First correct determination of oxygen permeability of cast ionomer from chronoamperometry on microelectrodes.
- More rigorous data analysis than in previous studies on oxygen permeability of polymer membranes.
- Factors responsible for changes of oxygen diffusion geometry through thin ionomer films identified.

ARTICLE INFO

Article history:
Received 1 March 2013
Received in revised form
20 June 2013
Accepted 22 June 2013
Available online 1 July 2013

Keywords:
Fuel cells
Oxygen reduction
6F-40
Diffusion coefficient
Shoup and Szabo equation

ABSTRACT

The paper presents a method for determination of diffusion coefficient and solubility of oxygen in cast polymer electrolyte from chronoamperometry of oxygen on polymer electrolyte coated platinum disk ultramicroelectrodes. The approach is based on numerical fitting of measured currents to the known but not previously used for polymer electrolytes equation derived by Shoup and Szabo. The method was applied to cast films of a novel polymer electrolyte 6F-40. As opposed to Nafion®, cast 6F-40 films do not undergo interfacial restructuring, i.e., they retain their original morphology under selected temperature and humidity conditions, which allows for accurate determination of both parameters from measurements for a range of electrode radii and film thicknesses. It is demonstrated that the Shoup and Szabo equation satisfactorily describes measured current transients for shorter oxygen reduction times, *i.e.*, when the diffusion field in the thin polymer film can be regarded as semiinfinite. The accuracy of the diffusion coefficient and solubility determinations was not measurably affected by the product water and the observed systematic changes of the fit quality in various time domains were attributed to approximate character of the fitting equation.

1. Introduction

Effective transport of oxygen to catalyst particles in polymer electrolyte fuel cells (PEFCs) is one of the key factors determining performance of the PEFC cathode. Therefore, oxygen permeabilities of Nafion® and alternative polymer electrolytes have been determined under various experimental conditions in numerous studies [1–10]. In many of those studies, chronoamperometry of the transport controlled oxygen reduction reaction (ORR) was measured in solid state electrochemical cells, where a disk shaped platinum ultramicroelectrode (UME) was pressed against a polymer electrolyte membrane in contact with humidified oxygen [9,10]. Assuming that the number of electrons participating in ORR was four, the method allowed for simultaneous determination of oxygen solubility (C_0) and diffusion coefficient (D), using the so called modified Cottrell equation [11]. However, the oxygen transport characteristics determined for preformed membranes [9,10] are expected to be different than those in the PEFC catalyst binders employing the same ionomer, as membrane manufacturing affects the polymer morphology [1,12]. On the other hand, studies utilizing solid state cells with Pt UMEs in contact with cast Nafion® films, whose morphology more closely resembles ionomer morphology in the catalyst layer, demonstrated interfacial restructuring of the polymer at the interface with smooth platinum surfaces [13–16]. The phenomenon results in the hydrophobic component of the ionomer being pushed out to its interface with bare Pt. Under such conditions, the apparent rate of ORR is reduced to such extent that the reduction current decreases even in the potential range where the reaction rate should be controlled exclusively by transport [13–16]. In consequence, the accuracy of a chronoamperometric determination of oxygen permeability is expected to progressively deteriorate with the reduction time. In this

* Tel.: +1 505 667 7192; fax: +1 505 665 4292.
E-mail addresses: jerzy@lanl.gov, j.chlistunoff@q.com.

0378-7753/$ – see front matter © 2013 Elsevier B.V. All rights reserved.
http://dx.doi.org/10.1016/j.jpowsour.2013.06.128

paper, we demonstrate a successful determination of the diffusion coefficient and solubility of oxygen in cast films of a novel, hydrocarbon based, proton-conducting polymer (6F-40) [17]. Cast films of 6F-40 retain their original morphology during ORR in a narrow range of temperature and humidity conditions, which makes it possible to measure transport controlled ORR currents unaffected by interfacial restructuring. In the data analysis, we used Shoup and Szabo equation [18], which offers a better current approximation than the modified Cottrell equation [11].

2. Experimental

The working electrode was either a 100 μm or a 50 μm diameter platinum microdisk electrode (Bioanalytical Systems). Before use, the microelectrode was polished with 0.25 μm diamond paste (Buehler) and 0.05 μm alumina (Buehler) and sonicated in deionized water (Millipore). Following multiple potential cycling between 0 V and 1.4 V vs. a hydrogen electrode (6% H_2 in Ar) in 0.5 mol dm^3 H_2SO_4, which resulted in the clean Pt surface, the microelectrode in the reduced state was removed from the solution, promptly rinsed with deionized water (Millipore) and the excess of water was removed with a stream of ultrahigh purity argon.

To recast the ionomer film, the electrode was held with the tip pointing up and a small volume of homemade 5% suspension of 6F-40 was deposited on the electrode with a micropipette. The electrode was then quickly turned and placed in a small volume ($\sim$5 cm^3) chamber filled with dry, ultrahigh purity Ar. Such a procedure guaranteed slow evaporation of the solvent and consequently a smooth film with a uniform thickness in its central portion, where the microdisk was located. The film thickness was measured by profilometry of a sample prepared in an identical way using an electrode that was not used in electrochemical experiments [14,15].

After the film dried out, the electrode was removed from the chamber and ribbons made of Nafion® 117 and of Pt were placed along the opposite sides of the glass body of the electrode. The ribbons were then secured with a Teflon tape, and electrolytic contacts between them and the film were made using small quantities of 6F-40 solution. In the minicell thus produced, the platinum ribbon served as a counter electrode and the Nafion® ribbon acted as an electrolytic bridge between the external reference electrode (6% H_2 in Ar/0.5 M H_2SO_4, $E = 39$ mV vs. RHE at sea level and 25 °C) and the working electrode (Fig. 1). Subsequently, the minicell was connected to the reference electrode and placed in a controlled humidity chamber (Fig. 1). In order to prevent gas exchange between the reference electrode and the controlled humidity chamber, the Nafion® ribbon passing through in the wall of the reference electrode tube was tightly covered with several layers of Teflon tape (Fig. 1). After that, film was cured for 24 h in argon at the desired temperature and humidity. Lithium chloride solutions (Fisher) of various concentrations were used to control the relative humidity during the film equilibration and the measurements. In order to attain the desired relative humidity (RH), the gas (argon or oxygen) was slowly passed through two large bubblers filled with a LiCl solution of the desired concentration before it entered the controlled humidity chamber partially filled with identical LiCl solution (Fig. 1). During the equilibration and measurements, the bubblers and the controlled humidity chamber were immersed in a controlled temperature water bath.

The electrochemical measurements were carried out with an EG&G PAR Model 283 potentiostat. Before the experiments, the electrode potential was cycled at 50 mV s^{-1} between 0 V and +1.4 V until a stable voltammogram was obtained. In order to provide a consistent electrode pretreatment and a clean Pt surface for every experiment, the microelectrode was held for 10 s at 1.4 V before a cathodic potential step or voltammetric scan was applied.

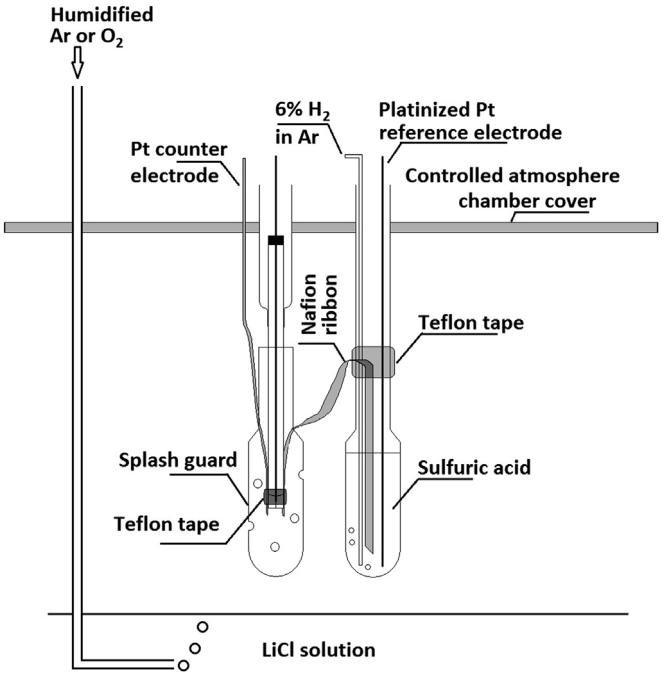

Fig. 1. Schematic of the electrochemical cell applied in the study.

3. Results and discussion

The top part of Fig. 2 shows a background corrected voltammogram of pure oxygen recorded at 60% relative humidity and 20 °C for a 100 μm Pt disk coated with a 26.5 μm thick film of 6F-40. Well-defined current plateaus that correspond to a transport controlled ORR can be seen in the forward and reverse scans of the voltammogram. The plateaus overlap at potentials $\leq$0.3 V, which indicates that the ORR is transport controlled in this potential range. Under the identical experimental conditions, a similar experiment for Nafion resulted in a voltammogram with a significantly narrower potential range, where the limiting currents in forward and reverse scans overlapped [14]. Non-existent or short current plateaus in oxygen voltammetry on ionomer-coated microelectrodes are demonstrated signs of ionomer restructuring [14]. The bottom portion of Fig. 2 shows plots of background corrected currents for transport controlled (0.1 V) ORR on 6F-40 coated electrodes at 60% relative humidity recorded under various experimental conditions and plotted versus the inverse square root of time. Irrespective of the film thickness (curves 1 and 3), size of the electrode (curves 1 and 5) and temperature (curves 4 and 5), the plots are essentially linear at shorter times of electrolysis (higher $t^{-1/2}$), whereas the current becomes essentially time independent at longer times. The approximately linear i vs. $t^{-1/2}$ dependence at shorter electrolysis times is consistent with the Shoup and Szabo equation [18] for a transport controlled reaction on an inlaid microdisk (semiinfinite diffusion field):

$$i = i_{ss}\left(0.7854 + 0.8862\tau^{-1/2} + 0.2146\exp\left(-0.7823\tau^{-1/2}\right)\right) \quad (1)$$

where i_{ss} is the steady state current corresponding to infinite reduction time (t) and τ is a dimensionless time variable equal to

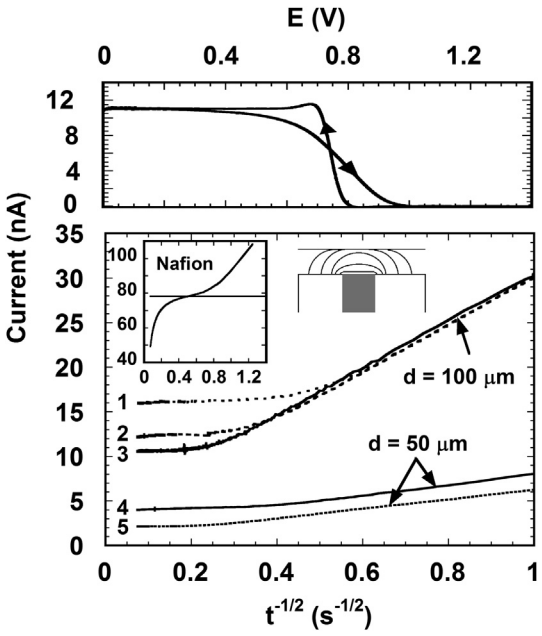

Fig. 2. Chronoamperometry (bottom part) and cyclic voltammetry (scan rate 5 mV s^{-1}, top part) of oxygen on 6F-40 coated Pt microelectrodes at 60% RH. Electrode diameter d (μm): 100 (plots 1–3), 50 (plots 4–5). Temperature: 40 °C (plots 1–4) and 20 °C (plot 5). Film thickness δ (μm): 8.0 (plot 1), 12.0 (plot 2), 26.5 (plots 3 and 5). Left inset in the bottom part: chronoamperometry of oxygen on Nafion® coated (δ = 16.5 μm) Pt microelectrode (d = 100 μm) at 0.1 V, 60% RH and 40 °C. Right inset in the bottom part: schematic presentation of the diffusion layer expansion during oxygen reduction on a film coated UME.

$4Dt/r^2$ (D is the diffusion coefficient of electroactive species and r is the microdisk radius). While Eq. (1) is non linear vs. $t^{-1/2}$, its actual departure from linearity is relatively insignificant under the conditions of the present experiments. For instance, the i/i_{ss} ratio calculated for 1380 equally spaced points between 1 s and 180 s using Eq. (1) with the parameters closely reflecting the characteristics of the present system, i.e., $D = 1 \times 10^{-7}$ cm^2 s^{-1}, r = 50 μm, could be fitted linearly with a correlation coefficient of 0.9997 and $\chi^2 = 0.7$. The steady state current (i_{ss}) for an inlaid disk is given by Ref. [19]:

$$i_{ss} = 4nFDC_0r \quad (2)$$

where F is the Faraday constant, n is the number of electrons, D is the diffusion coefficient, and C_0 is bulk concentration of the electroactive species. In accordance with Eq. (2), we found that the steady state currents ($i_{ss} = \lim_{t\to\infty}(i)$) obtained from the numerical fitting of the experimental data using Eq. (1) for the 100 μm and 50 μm electrodes under identical experimental conditions remained in the approximate ratio 2:1, as expected from the corresponding ratio of the electrode radii (100 μm:50 μm). A similar conclusion can be reached from a linear extrapolation of plots 13 and 4 (see Fig. 2) to zero. From Eq. (1), on the other hand, one can demonstrate that the ratio of the currents measured for the 100 μm and 50 μm electrodes in the limit of very short times ($t^{-1/2} \to \infty$) should be equal to the ratio of squares of the electrode radii, i.e., 4. As seen in Fig. 2, the ratio of the respective currents (plots 13 and 4) at $t^{-1/2} = 1$ is already close to 4 (~3.8).

The short time behavior is easily understandable if one realizes that a purely hemispherical diffusion requires time to develop (Eq. (1)) and diffusion at the very beginning of the electrolysis is predominantly planar. Under such conditions, the ratio of 4 is also predicted by Cottrell equation [20], which describes purely planar diffusion controlled processes.

According to Eq. (1), the time required for the current to reach its steady state value is indefinitely long. However, there exists another limitation in the present case, which prevents the measured current from reaching its steady state value corresponding to the purely hemispherical diffusion field (Eq. (2)). This factor is associated with a finite thickness of the polymer electrolyte layer. During electrolysis, the diffusion field is expanding, which causes a decrease of the concentration gradient of the electroactive species (oxygen) and current decay. In the present case, when the boundary of the diffusion field reaches the film boundary, the decrease of the diffusion rate significantly slows down as the diffusion field can now expand only in the direction parallel to the electrode surface. The current is now dominated by the highest concentration gradient, perpendicular to the electrode surface, and therefore becomes virtually independent of time. The development of the oxygen diffusion field is schematically depicted in the right inset in Fig. 2. The film thickness (δ) is a crucial factor determining the time when the current starts stabilizing as well as its magnitude. As expected, the thinner the film the sooner the current stabilizes and the higher it is (Fig. 2, curves 1–3). The steady state current originating from such phenomena will be called hereafter $i_{ss}(\delta)$. While the thin layer component to $i_{ss}(\delta)$ is quite significant, the diffusion of oxygen from the cylindrical volume surrounding the microdisk is not negligible, either. One can see (Fig. 2) that $i_{ss}(\delta)$ is not inversely proportional to δ, as would be expected for purely planar thin layer diffusion. It can also be shown that even for the lowest applied ratio (0.08) of film thickness (δ = 8 μm) to electrode diameter (d = 100 μm), the steady state currents ($i_{ss}(\delta)$) are higher by some 40% than those expected for thin layer planar diffusion ($nF\pi r^2DC_0/\delta$). The observed behavior of oxygen on 6F-40 coated Pt is contrasted by that on Nafion® coated Pt under similar conditions (see left inset, Fig. 2). Significantly higher ORR currents observed for Nafion® indicate its higher oxygen permeability compared to that of 6F-40. However, Nafion® undergoes restructuring on Pt surface [14–16], which causes electrode surface blocking and time dependent ORR current losses [14]. Such behavior is seen in the left inset in Fig. 2, which shows an oxygen reduction current measured using a Nafion® coated (δ = 16.5 μm) Pt microelectrode (d = 100 μm) at 60% RH and 40 °C. The time of the electrolysis for both Nafion (inset) and 6F-40 coated electrodes was 180 s. It is seen that the current on the Nafion® coated electrode tends to stabilize close to the respective voltammetric limiting current, but eventually significantly decreases, which is yet another sign of Nafion® restructuring [14]. For comparison, the voltammetric limiting current measured under the identical conditions for a 26.5 μm thick 6F-40 film and the respective $i_{ss}(\delta)$ (plot 3, Fig. 2) is identical. Moreover, as opposed to the Nafion® film (inset), $i_{ss}(\delta)$ for the 6F-40 film remains stable during the entire reduction time (180 s). The same was true for the thinner (8 μm and 16 μm) 6F-40 films and the smaller (50 μm) microelectrode at 60% RH and 20 °C–40 °C (Fig. 2). Unfortunately, at higher temperatures and humidities, 6F-40 was found susceptible to restructuring too, which limited the range of conditions, where ORR on 6F-40 coated electrodes could be regarded as undistorted by restructuring phenomena.

While non-planar diffusion is a complicating factor for solving the second Fick's law in electrochemical systems, it offers a unique opportunity to simultaneously determine solubility (C_0) and diffusion coefficient (D) of an electroactive species when the number of electrons is known. In the present case, both parameters can be determined by numerical fitting of the experimental i vs. $t^{-1/2}$ plots (Fig. 2) using Eq. (1). In the past, these parameters were determined for preformed membranes [1–10] using the modified Cottrell equation [11]. While an equivalence has been demonstrated between Eq. (1) (Shoup and Szabo equation) and the

modified Cottrell equation [11] for liquid solutions under limited experimental conditions [21], it has to be stressed that such an equivalence cannot be considered general. This is because the length of time, where the Cottrell equation approximately holds during chronoamperometry on microelectrodes, does depend on the diffusion coefficient of the electroactive species and the electrode size, which both determine the actual fraction of hemispherical diffusion component in a transport controlled current. As the Shoup and Szabo equation is a higher order approximation of that current, it is recommended for analysis of oxygen chronoamperometry on ionomer coated microelectrodes, where the film thickness, the electrode diameter and the actual permeation parameters affect the time domain, where oxygen diffusion may be considered semi-infinite.

Fig. 3 shows plots of D, C_0, and permeability (DC_0) vs. inverse square root of time ($t^{-1/2}$) determined from a single chronoamperometric experiment together with the respective χ^2 plot, obtained from numerical fitting of the experimental data using Eq. (1) for different time ranges extending from 1 s to longer reduction times (t) and assuming $n = 4$. The plots demonstrate presence of systematic changes of all above parameters. For $t \leq 10$ s ($t^{-1/2} \geq 0.32$ s$^{-1/2}$), D and DC_0 increase, whereas C_0 decreases with $t^{-1/2}$. Opposite trends are observed at $t^{-1/2} \leq 0.32$ s$^{-1/2}$, where $t^{-1/2} = 0.32$ s$^{-1/2}$ roughly corresponds to the moment, when the diffusion layer boundary reaches that of the film (see Fig. 2 and also the respective χ^2 plot in Fig. 3). The trends at $t^{-1/2} \leq 0.32$ s$^{-1/2}$ ($t \geq 10$ s) result from obvious inapplicability of Eq. (1), which was derived for infinite diffusion conditions, to the limited diffusion field conditions that emerge at $t > 10$ s. The changes in D, C_0, and DC_0 at $t^{-1/2} \geq 0.32$ s$^{-1/2}$ reflect either systematic departures of the system from the assumptions used to derive Eq. (1) or the approximate character of Eq. (1) itself. Among most likely reasons for non-ideal system behavior are changes in D, C_0 and possible partial hydrogen peroxide generation. Such changes might result from an increase in the film hydration during electrolysis caused by the product water. For the film that does not undergo interfacial restructuring, an increase in the film hydration is expected to lead to increases in DC_0 [1] and n (decrease in peroxide generation) [22].

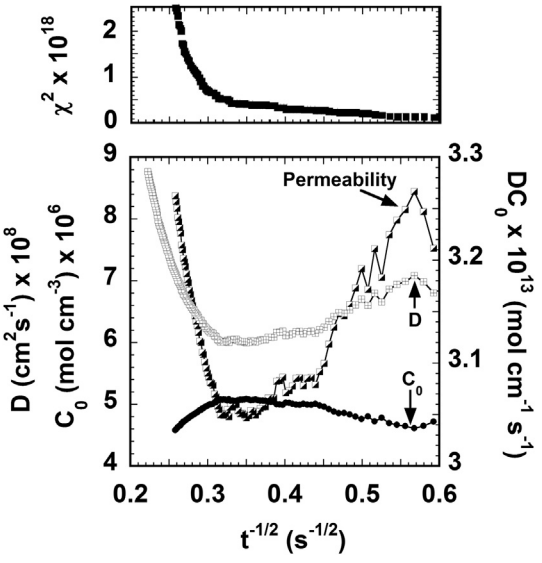

Fig. 3. Bottom part: diffusion coefficient (D), solubility (C_0) and permeability of oxygen (DC_0) obtained from numerical fitting of a single chronoamperometric transient using Shoup and Szabo equation (Eq. (1)) in various time ranges between 1 s and longer reduction times (t). Relative humidity 60%. Temperature 20 °C. Electrode diameter 100 μm. Film thickness 26.5 μm. Top part: fit quality illustrated by the corresponding χ^2 parameter.

As the parameters D, C_0, and n are strongly interrelated, it is difficult to predict the effect of their changes on the fitting of experimental data using Eq. (1). Consequently, a number of calculations of ORR current were performed, where n and DC_0 were systematically varied. In the calculations it was assumed that both n and DC_0 increase with time, as expected from the amount of water generated [1,22]. We assumed that both parameters increased linearly with the concentration of water generated. The latter was computed from the electrolysis charge and an approximate diffusion layer volume (thickness). While the exact function describing the changes of n and DC_0 is not known, it is intuitively understood that the current at very short times should be virtually undistorted by the product water, whereas at longer times it should be higher than predicted due to increases in both n [22] and DC_0 [1]. This should lead to lower average slopes of i vs. $t^{-1/2}$ relationships, which was demonstrated by the calculations. Subsequently, the theoretical i vs. $t^{-1/2}$ relationships were fitted using Eq. (1). The numerical fitting of the data revealed that the observed changes in D and C_0 for $t^{-1/2} \geq 0.32$ s$^{-1/2}$ (Fig. 3) cannot be explained by changes in film hydration during electrolysis, in agreement with quite low ORR currents. Moreover, unless the water transport from the electrode surface was severely hindered, the highest concentrations of water would be expected in the immediate vicinity of the electrode surface and would be on the order of bulk oxygen concentrations, *i.e.*, no more than a few millimolar. At the same time, water concentrations in the hydrophilic domains of hydrated ionomers are higher by orders of magnitude. Consequently, the observed small changes in D and C_0 (Fig. 3) most likely result from approximations used to derive Eq. (1). Note that the very decrease in DC_0 with time (Fig. 3) is by itself inconsistent with the expected effects of water generated on oxygen permeability. Interestingly, application of the most recent solution of the second Fick's law for an inlaid microdisk [23] resulted in lower quality fits (higher χ^2) of the experimental data.

Overall, as the time dependences of D, C_0, and DC_0 for $t^{-1/2} \geq 0.32$ s$^{-1/2}$ are rather weak (within ~10%), the method applied for their determination is considered reliable. The numerical values for all parameters determined from multiple experiments within the widest time ranges corresponding to undisturbed infinite diffusion field are summarized in Table 1.

The significantly lower oxygen permeability of 6F-40 in comparison to that of Nafion® is quite striking and may suggest different factors controlling oxygen transport in both ionomers. For instance, oxygen transport in the current experiments may be controlled by diffusion of H^+, which participates in ORR. The extremely low values of D in Table 1 seem inconsistent with such an explanation, but the almost identical values of ionic conductivities of Nafion® (111 mS cm^{-1}) and 6F-40 (92 mS cm^{-1}) [17] provide a

Table 1
6F-40 oxygen permeation properties determined from chronoamperometry.[a]

	20 °C, 60% RH		40 °C, 60% RH	
	2100 m above sea level	At sea level[b]	2100 m above sea level	At sea level[b]
Solubility × 10^6 (mol cm^{-3})	7.6 ± 0.8	9.8 ± 1.0	4.6 ± 0.2	6.0 ± 0.3
Diffusion coefficient × 10^8 (cm^2 s^{-1})	4.5 ± 0.7	4.5 ± 0.7	12.5 ± 1.0	12.0 ± 1.0
Permeability × 10^{13} (mol cm^{-1} s^{-1})	3.0 ± 0.2	4.4 ± 0.3	5.5 ± 0.2	7.1 ± 0.3

[a] Errors are standard deviations of the mean.
[b] Data obtained at 2100 m above sea level (Los Alamos elevation). Altitude correction calculated from Henry's law ($C_0 = Kp_{O_2}$, where K is Henry's constant and p_{O_2} is atmospheric pressure of oxygen).

definite proof that H^+ diffusion cannot be responsible for oxygen transport in 6F-40 under ORR conditions.

4. Conclusions

The present results demonstrate that chronoamperometry of oxygen in solid state cells employing platinum ultramicroelectrodes coated with cast polymer electrolyte films is a convenient and accurate method of determination of oxygen diffusion coefficients and solubilities in such electrolytes, provided the polymer does not undergo interfacial restructuring [13–16] during electrolysis. The method might also be helpful in detecting possible effects of H^+ transport on diffusion controlled oxygen reduction currents.

Acknowledgments

Thanks are due to Dr. Yu Seung Kim who kindly provided a sample of 6F-40 solution and to the DOE Office of Energy Efficiency and Renewable Energy for financial support.

References

[1] K. Broka, P. Ekdunge, Journal of Applied Electrochemistry 27 (1997) 117–123.
[2] L. Zhang, C. Ma, S. Mukerjee, Electrochimica Acta 48 (2003) 1845–1859.
[3] L. Zhang, C. Ma, S. Mukerjee, Journal of Electroanalytical Chemistry 568 (2004) 273–291.
[4] V.I. Basura, P.D. Beattie, S. Holdcroft, Journal of Electroanalytical Chemistry 458 (1998) 1–5.
[5] P.D. Beattie, V.I. Basura, S. Holdcroft, Journal of Electroanalytical Chemistry 468 (1999) 180–192.
[6] V.I. Basura, C. Chuy, P.D. Beattie, S. Holdcroft, Journal of Electroanalytical Chemistry 501 (2001) 77–88.
[7] A. Parthasarathy, S. Srinivasan, A.J. Appleby, C.R. Martin, Journal of the Electrochemical Society 139 (1992) 2530–2537.
[8] A. Parthasarathy, S. Srinivasan, A.J. Appleby, C.R. Martin, Journal of the Electrochemical Society 139 (1992) 2856–2862.
[9] F.N. Büchi, M. Wakizoe, S. Srinivasan, Journal of the Electrochemical Society 143 (1996) 927–932.
[10] A. Parthasarathy, C.R. Martin, S. Srinivasan, Journal of the Electrochemical Society 138 (1991) 916–921.
[11] K. Aoki, J. Osteryoung, Journal of Electroanalytical Chemistry 125 (1981) 315.
[12] J.A. Elliott, S. Hanna, J.N. Newton, A.M.S. Elliott, G.E. Cooley, Polymer Engineering & Science (2006) 228–234.
[13] F.A. Uribe, T.E. Springer, S. Gottesfeld, Journal of the Electrochemical Society 139 (1992) 765–773.
[14] J. Chlistunoff, F. Uribe, B. Pivovar, ECS Transactions 1 (6) (2006) 137–146.
[15] J. Chlistunoff, F. Uribe, B. Pivovar, ECS Transactions 2 (8) (2007) 37–46.
[16] D.L. Wood III, J. Chlistunoff, J. Majewski, R.L. Borup, Journal of the American Chemical Society 131 (2009) 18096–18104.
[17] Y.S. Kim, B. Einsla, M. Sankir, W. Harrison, B.S. Pivovar, Polymer 47 (2006) 4026–4035.
[18] D. Shoup, A. Szabo, Journal of Electroanalytical Chemistry 140 (1982) 237–245.
[19] Y. Saito, Review of Polarography (Japan) 15 (1968) 177–187.
[20] F.G. Cottrell, Zeitschrift für Physikalische Chemie 42 (1903) 385–431.
[21] L. Xiong, L. Aldous, M.C. Henstridge, R.G. Compton, Analytical Methods 4 (2) (2012) 371.
[22] J. Chlistunoff, B. Pivovar, ECS Transactions 11 (1) (2007) 1115–1125.
[23] A. Meena, L. Rajendran, Russian Journal of Electrochemistry 47 (2011) 147–155.